

---

# Binary phase elements: optical and statistical properties

M.V.Shovgenyuk, T.Ye.Krokhmalskii, M.P.Kozlovskii

Institute for Condensed Matter Physics  
of the National Academy of Sciences of Ukraine  
1 Svientsitskii Str., 79011, L'viv, Ukraine, E-mail: mv@icmp.lviv.ua

Received 12.03.2001

## Abstract

The optical properties of binary phase elements (BPE) are described by using the method of coordinate-frequency distribution of signals. The analytical expressions for the autocorrelation function and the Wiener spectrum of the BPE spatial frequencies are obtained. On their basis the generalized optical parameter for a quantitative estimation of the level of optical noise and the fluctuation of the intensity of the Wiener spectrum interference pattern is calculated. A statistical description of the phase elements is suggested, on the basis of which the parameter of non-orthogonality is introduced. It characterizes the binary phase distribution for the classes of orthogonal, quasi-orthogonal and random phase elements. A diagram representation (optical parameter vs non-orthogonality parameter) for the description of the classes of orthogonal, quasi-orthogonal and random phase elements is introduced.

**Key words:** image processing, phase masks, signal/noise ratio

**PACS:** 42.30.Va; 42.79.-e; 42.79.Hp

## Contents

<b>1. Introduction</b>	<b>2</b>
<b>2. Description of the optical properties of the binary phase elements</b>	<b>3</b>
2.1. Definition of the BPE . . . . .	3
2.2. The basic functional of the coordinate-frequency distribution . . . . .	3
2.3. The coordinate-frequency distribution of the BPE . . . . .	4
2.4. The Wiener spectrum of the spatial frequencies of the BPE . . . . .	5
<b>3. Typical optical schemes</b>	<b>5</b>
3.1. Joint transform correlator . . . . .	5
3.2. Hadamard-Schur multiplication in the $4\mathbf{f}_0$ scheme . . . . .	7
<b>4. Classes of the binary phase elements</b>	<b>9</b>
4.1. Orthogonal BPE . . . . .	9
4.2. Collinear BPE . . . . .	11
4.3. Random BPE . . . . .	12
4.4. Randomization of the ordered phase elements . . . . .	12
4.5. Quasi-orthogonal BPE . . . . .	13

4.6. Quasi-collinear BPE . . . . .	14
<b>5. The generalized optical parameter</b>	<b>14</b>
5.1. Optical noise level . . . . .	16
<b>6. Two-parametric representation</b>	<b>16</b>
6.1. Relation between the classes of the orthogonal and collinear phase elements . . .	16
6.2. Two-parameter representation of the properties of the different classes of the BPE	18
<b>7. Conclusions</b>	<b>19</b>

## 1. Introduction

The use of the binary phase elements permits to increase essentially the efficiency of the holographic system for image recognition [1–4, 6, 7, 9]. The most popular for such system becomes the binary optical elements with random distribution of phase called in [1] the random phase masks.

In the paper by Javidi and Horner [2] the security verification technique was realized for the first time. This method is based on the exploiting of the random phase masks as the input image in the optical correlator [5]. This method was modified and experimentally verified in the [3]. The study of the influence of the structure of the random phase mask on the Wiener spectrum of spatial frequencies and on the behaviour of the autocorrelation function shows that the random binary phase masks have a series of advantages in comparison with the amplitude masks, particularly, they have a low noise level.

The holographic image recognitions by using the random phase masks were studied in the paper [4]. Besides the binary masks, the masks with multilevel phase shift of certain elements were examined [6–9]. However, there was not any systematic approach to the study of the properties of different types of binary phase masks.

Although the main attention was paid to the phase elements with random phase distribution, it is worth to note that for tasks of image recognition a wider class of phase elements having certain symmetrical or structural properties may be used. In particular, one may use such phase elements constructed on the basis of the Hadamard orthogonal matrices [10–12]. In our previous paper [13] we have suggested a statistical approach to the

description of a wide class of quasi-orthogonal phase elements, which contains both the completely ordered (with respect to orthogonality criteria) phase elements and the random phase elements.

In the present paper the method of coordinate-frequency distribution of signals (CFDS) [16–19] is elaborated to the description of the binary phase elements with an arbitrary phase distribution. The idea of this method is to construct the CFDS functional which permits to describe self-consistently the properties of the optical element both in the coordinate and frequency planes. We have obtained the analytical expressions for the autocorrelation function and the Wiener spectrum. We have performed numerical calculations of the optical properties of different types of phase masks.

We have suggested a systematic statistical approach to study a wide class of the binary phase elements including the random phase masks [28]. We have proved that the non-orthogonality parameter introduced in paper [13] permits within the frames of a unique approach to describe the properties of both the quasi-orthogonal and quasi-collinear binary phase masks. It is shown that every class is characterized by the statistical description of the non-diagonal elements of a matrix  $\mathbf{S}$ , constructed from the scalar products of the rows (columns) of the initial matrix of phase elements. It is found that during the process of randomization of the ordered phase elements the  $\delta$ -like peaks are transformed into Gaussian curves that become broader and are transformed into the Gaussian distribution of random masks. A two-parameter representation of the properties of different classes of the BPE is suggested.

## 2. Description of the optical properties of the binary phase elements

### 2.1. Definition of the BPE

Consider the plane rectangle phase element consisting of  $N \times M$  identical elementary cells of the sizes  $T_x \times T_y$ . The transmission function of a separate cell with the coordinates  $n, m$  has the form

$$t_{n,m}(x, y) = \text{rect}\left(\frac{x}{T_x}\right) \text{rect}\left(\frac{y}{T_y}\right) \times \exp(i\pi\phi(n, m)), \quad (1)$$

where  $\text{rect}(x/T_x)$  is the rectangle pulse [14].

The distribution of the complex amplitude of the light wave on the exit of such an element is given by the following function [13, 28]

$$f(x, y) = \sum_{n=1}^N \sum_{m=1}^M \text{rect}\left(x - \left[n - \frac{N+1}{2}\right] T_x\right) \times \text{rect}\left(y - \left[m - \frac{M+1}{2}\right] T_y\right) \times \exp(i\pi\Delta\phi(n, m)), \quad (2)$$

that, generally speaking, does not split with respect to the variables  $x$  and  $y$ . Every elementary cell changes the phase of an incident plane wave by the quantity  $\Delta\phi(n, m) = \phi(n, m) - \phi_0$ , where  $\phi_0$  is constant. In what (such?) follows we shall consider the phase elements, the elementary cellof which changes the phase by the quantity  $\Delta\phi(n, m) = 0; 1$ .

Then the distribution of the phase is completely described by the matrix

$$\mathbf{A} = [A_{nm}], \quad (3)$$

where the coefficients  $A_{nm}$  take values  $+1; -1$ . As a result the function (2) is real, i.e.  $f^*(x, y) \equiv f(x, y)$ . The phase elements described by formulae (2), (3), will be called *the binary phase elements*.

In Fig. 1 we have displayed the typical cases of different classes of the binary phase elements which will be described in Section 4.

On the basis of the definition (1)-(3), the Fourier-spectrum of the binary phase element can be presented in the form of the product

$$F(\omega_x, \omega_y) = F_0(\omega_x)F_0(\omega_y)\Phi(\omega_x, \omega_y) \quad (4)$$

Here

$$F_0(\omega_x)F_0(\omega_y) = \text{sinc}\left(\frac{T_x\omega_x}{2\pi}\right) \text{sinc}\left(\frac{T_y\omega_y}{2\pi}\right)$$

is the Fourier spectrum of the elementary cell (1). The function

$$\Phi(\omega_x, \omega_y) = C_{NM}(\omega_x, \omega_y) \sum_{n=1}^N \sum_{m=1}^M A_{nm} \times \exp[-i(nT_x\omega_x + mT_y\omega_y)] \quad (5)$$

describes the Fourier-spectrum of the phase distribution. The presence of the factor

$$C_{NM}(\omega_x, \omega_y) = \exp\left[i\left(\frac{N+1}{2}T_x\omega_x + \frac{M+1}{2}T_y\omega_y\right)\right] \quad (6)$$

is connected with the chosen reference frame in the centre of the phase element of an arbitrary size (see (2)).

### 2.2. The basic functional of the coordinate-frequency distribution

Let us construct the coordinate-frequency distribution (CFD) for the phase element (2). As a definition of such distribution, let us take the functionals in the form of the Woodward ambiguity function [16]:

the coordinate representation:

$$\mathcal{W}_{f_1 f_2^*}(\mathbf{r}_0; \omega_0) = \int_{-\infty}^{\infty} \mathbf{f}_1\left(\mathbf{r} + \frac{\mathbf{r}_0}{2}\right) \mathbf{f}_2^*\left(\mathbf{r} - \frac{\mathbf{r}_0}{2}\right) \times \exp(-i\omega_0 \mathbf{r}) d\mathbf{r}, \quad (7)$$

the space-frequency representation:

$$\mathcal{W}_{F_1 F_2^*}(\omega_0; \mathbf{r}_0) = \frac{1}{(2\pi)^2} \int_{-\infty}^{\infty} F_1\left(\boldsymbol{\Omega} + \frac{\omega_0}{2}\right) F_2^*\left(\boldsymbol{\Omega} + \frac{\omega_0}{2}\right) \times \exp(i\mathbf{r}_0 \boldsymbol{\Omega}) d\boldsymbol{\Omega}, \quad (8)$$

where  $F_1(\omega), F_2(\omega)$  are the Fourier transforms of the functions  $f_1(\mathbf{r})$  and  $f_2(\mathbf{r})$ , respectively.

For the functionals (7)-(8), the theorem of identity is valid [16]

$$\mathcal{W}_{f_1 f_2^*}(\mathbf{r}_0; \omega_0) \equiv \mathcal{W}_{F_1 F_2^*}(\omega_0; \mathbf{r}_0). \quad (9)$$

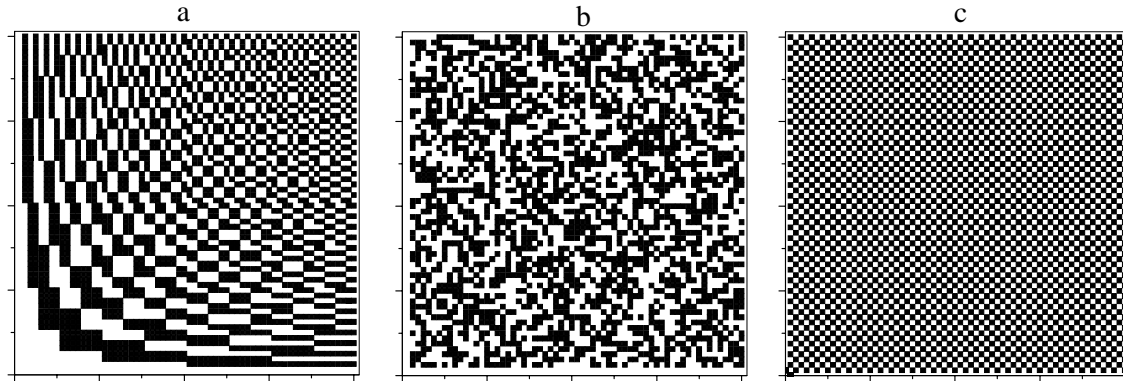


**Fig. 1.** Different types of the binary phase elements: a) - the canonical Hadamard matrix; b) - random matrix; c) - chess-like matrix.

We used the distribution functions for denoting the form of representation of the functional, as the indices, and a sequence of conjugate coordinates  $\mathbf{r}_0$  and  $\omega_0$ , as the arguments (the former is the proper coordinate of the distribution).

The exploiting of the method of distribution of signals allows one to describe the optical properties of the elements of optical schemes both in the coordinate and frequency planes.

Using the distribution (7) under the condition  $\mathbf{r}_0 = \mathbf{0}$  with the help of the operator of the inverse Fourier transformation  $\hat{\mathcal{F}}^{-1}$  according to *direct scheme* one can uniquely and completely reproduce the intensity of the diffracted light

$$\hat{\mathcal{F}}^{-1} \{W_{ff^*}(0; \omega_0)\} = |f(\mathbf{r})|^2. \quad (10)$$

On the contrary, if  $\omega_0 = \mathbf{0}$ , the Wiener (power) spectrum of the spatial frequencies can be restored by using the operator of the direct Fourier transform  $\hat{\mathcal{F}}$  according to *the inverse scheme*

$$\hat{\mathcal{F}} \{W_{FF^*}(0; \mathbf{r}_0)\} = |F(\omega)|^2. \quad (11)$$

### 2.3. The coordinate-frequency distribution of the BPE

To construct the coordinate-frequency distribution of the binary phase element, let us use the spatial-frequency representation (8). From equation (4), one can write the general expression for the coordinate-frequency distribution of the binary phase element in

the form of an expansion with respect to the shifted functionals of the elementary cells  $\mathcal{W}_{F_0 F_0^*}(\omega_{0x}; x_0 - kT_x) \mathcal{W}_{F_0 F_0^*}(\omega_{0y}; y_0 - lT_y)$ :

$$\begin{aligned} \mathcal{W}_{FF^*}(\omega_{0x}, \omega_{0y}; x_0, y_0) = \\ C_{NM} \sum_{k=-(N-1)}^{N-1} \sum_{l=-(M-1)}^{M-1} Q_{kl}^{(1)}(\omega_{0x}, \omega_{0y}) \\ \times \mathcal{W}_{F_0 F_0^*}(\omega_{0x}; x_0 - kT_x) \\ \times \mathcal{W}_{F_0 F_0^*}(\omega_{0y}; y_0 - lT_y), \end{aligned} \quad (12)$$

where

$$\begin{aligned} Q_{kl}^{(1)}(\omega_{0x}, \omega_{0y}) = \sum_{n=1}^{N-k} \sum_{m=1}^{M-l} A_{n+k} A_{m+l} A_n \\ \times \exp \left\{ -i \left[ \left( n + \frac{k}{2} \right) T_x \omega_{0x} \right. \right. \\ \left. \left. + \left( m + \frac{l}{2} \right) T_y \omega_{0y} \right] \right\}. \end{aligned} \quad (13)$$

The multiplier  $C_{NM} = C_{NM}(\omega_{0x}, \omega_{0y})$  is given by (6). The analytical derivation of formulae (12)-(13) can be found in the paper presented by the authors [28].

The frequency functions (13) are determined only through the binary distribution of the phase and their form coincide with the definition of the basis functional distribution (7).

The main peculiarity of the functional of phase distribution is that such a distribution is discrete and continuous: it is discrete with respect to indices  $k$  and  $l$  (i.e. with respect to coordinates) and continuous with respect to spatial frequency  $\omega_0(\omega_{0x}, \omega_{0y})$ . However, it can not be reduced to the symmetric form

(7) since the indices of summation are integer numbers.

In the paper [16] for the coordinate-frequency distribution of the rectangle pulse the following formula was derived

$$\begin{aligned} \mathcal{W}_{f_0 f_0^*}(x_0; \omega_0) = & \\ & \frac{\sin\left(\frac{\omega_0}{2}[T_x + x_0]\right)}{\frac{\omega_0 T_x}{2}} \operatorname{rect}\left(\frac{T_x + 2x_0}{2T_x}\right) \\ & + \frac{\sin\left(\frac{\omega_0}{2}[T_x - x_0]\right)}{\frac{\omega_0 T_x}{2}} \operatorname{rect}\left(\frac{T_x - 2x_0}{2T_x}\right). \end{aligned} \quad (14)$$

With the help of (14) one can easily obtain the coordinate-frequency distribution of the elementary cell (1).

#### 2.4. The Wiener spectrum of the spatial frequencies of the BPE

Let us use the inverse scheme of restoration (11). As a result, the following formula holds for the Wiener spectrum of the spatial frequencies of the phase element:

$$|F(\omega_x, \omega_y)|^2 = |F_0(\omega_x)F_0(\omega_y)|^2 \mathcal{M}(\omega_x, \omega_y), \quad (15)$$

where the modulation function  $\mathcal{M}(\omega_x, \omega_y)$  (it is determined only by the binary phase distribution) has the form of the two-dimensional Fourier expansion [13]

$$\begin{aligned} \mathcal{M}(\omega_x, \omega_y) = & Q_{00}^{(1)} \\ & + 2 \left\{ \sum_{k=1}^{N-1} Q_{k0}^{(1)} \cos \omega_x k T_x + \sum_{l=1}^{M-1} Q_{0l}^{(1)} \cos \omega_y l T_y \right. \\ & + \sum_{k=1}^{N-1} \sum_{l=1}^{M-1} \left[ Q_{kl}^{(1)} \cos(\omega_x k T_x + \omega_y l T_y) \right. \\ & \left. \left. + Q_{kl}^{(2)} \cos(\omega_x k T_x - \omega_y l T_y) \right] \right\}. \end{aligned} \quad (16)$$

We consider two types of the Fourier coefficients

$$\begin{aligned} Q_{kl}^{(1)} = Q_{kl}^{(1)}(0, 0) = & \\ & \sum_{n=1}^{N-k} \sum_{m=1}^{M-l} A_{n+k} A_{m+l} A_{nm}, \\ Q_{kl}^{(2)} = Q_{kl}^{(2)}(0, 0) = & \\ & \sum_{n=1}^{N-k} \sum_{m=1}^{M-l} A_{n+k} A_{m+l} A_{nm}, \end{aligned} \quad (17)$$

which according to the definition (13) for  $k < 0$  or  $l < 0$  are connected by the relations

$$Q_{-kl}^{(1)} = Q_{kl}^{(2)}; \quad Q_{k-l}^{(1)} = Q_{kl}^{(2)}. \quad (18)$$

The modulation function has a series of peculiarities. For an arbitrary phase distribution, the Fourier coefficients  $Q_{kl}^{(1)}$  and  $Q_{kl}^{(2)}$  are always equal to an integer number, however  $\mathcal{M}(\omega_x, \omega_y) \geq 0$ . The spectrum of  $\mathcal{M}(\omega_x, \omega_y)$  is discrete with a sequence of frequencies  $\Omega_n = 2\pi n/T_x$ ,  $n = 0 \div (N-1)$   $\Omega_m = 2\pi m/T_y$ ,  $m = 0 \div (M-1)$ , respectively. The upper spatial frequencies  $\Omega_{N-1}$  and  $\Omega_{M-1}$  are determined by the sizes  $N$  and  $M$  of the phase element.

### 3. Typical optical schemes

On the basis of the method of distribution of signals let us describe typical optical schemes having as an input the phase element which is described by the coordinate-frequencies distribution  $\mathcal{W}_{ff^*}(\mathbf{r}_0; \omega_0)$ . Generally speaking, the formation of the diffracted amplitude  $g_1(\mathbf{r})$  on the output of the cascade is given by the distribution

$$\begin{aligned} \mathcal{W}_{g_1 g_1^*}(\mathbf{r}_0; \omega_0) = & \\ & \mathcal{W}_{ff^*}(a_{11}\mathbf{r}_0 + \mathbf{a}_{12}\omega_0; \mathbf{a}_{21}\mathbf{r}_0 + \mathbf{a}_{22}\omega_0). \end{aligned} \quad (19)$$

From equation (19) one can see that a linear transformation of the conjugate coordinates  $(\mathbf{r}_0; \omega_0)$  of the distribution of the input signal is described by the matrix  $\mathbf{M} = [a_{ij}]$ .

Let us examine two typical optical schemes containing the binary phase elements.

#### 3.1. Joint transform correlator

Let us describe a scheme (Fig. 2) of the joint transform correlator (JTC) [5], having the binary phase element in the input

$$f(x, y) = f_1(x, y + b) + f_2(x, y - b). \quad (20)$$

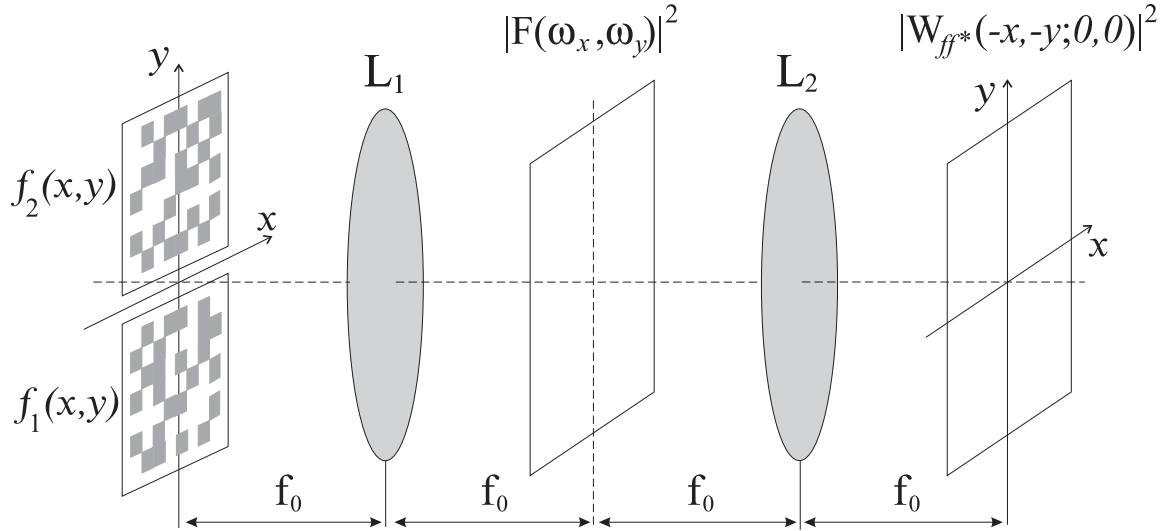


**Fig. 2.** Joint transform correlator.

The coordinate-frequency distribution of such signal is given by

$$\begin{aligned} \mathcal{W}_{ff^*}(x_0, y_0; \omega_{0x}, \omega_{0y}) = & \\ \mathcal{W}_{f_1 f_1^*}(x_0, y_0; \omega_{0x}, \omega_{0y}) \exp(+ib\omega_{0y}) & \\ + \mathcal{W}_{f_2 f_2^*}(x_0, y_0; \omega_{0x}, \omega_{0y}) \exp(-ib\omega_{0y}) & \\ + \mathcal{W}_{f_1 f_2^*}(x_0, y_0 + 2b; \omega_{0x}, \omega_{0y}) & \\ + \mathcal{W}_{f_2 f_1^*}(x_0, y_0 - 2b; \omega_{0x}, \omega_{0y}). & \end{aligned} \quad (21)$$

In the first cascade of the JTC an exact condition of the Fourier transform that is given by the matrix

$$\mathbf{M} = \begin{bmatrix} 0 & -\frac{f_0}{\kappa} \\ \frac{\kappa}{f_0} & 0 \end{bmatrix}, \quad (22)$$

( $\kappa = 2\pi/\lambda$  is the wave number,  $\lambda$  is the light wave length,  $f_0$  is the focal distance) is realized. Thus in the frequency plane one gets the distribution

$$\mathcal{W}_{g_1 g_1^*}(\mathbf{r}_0; \omega_0) = \mathcal{W}_{ff^*} \left( -\frac{f_0}{\kappa} \omega_0; \frac{\kappa}{f_0} \mathbf{r}_0 \right). \quad (23)$$

Putting  $\mathbf{r}_0 = \mathbf{0}$  according to the direct scheme (10) one gets the joint Wiener spectrum of the spatial frequencies of two phase elements

$$|g_1(\mathbf{r})|^2 = \frac{1}{(\lambda f_0)^2} \left| F \left( \frac{\kappa}{f_0} \mathbf{r} \right) \right|^2. \quad (24)$$

Let us note that this is equivalent (see Subsection 2.4.) to an application of the inverse restoration scheme for the coordinate-frequency distribution of the input signal (11).

The Wiener spectrum (24) produced as an output of the first cascade is the input signal for the second cascade of the JTC. The coordinate-frequency distribution of such signal has the form

$$\begin{aligned} \mathcal{W}_{|g_1|^2 |g_1|^2}(\mathbf{r}_0; \omega_0) = & \frac{1}{(2\pi)^2} \\ \times \int_{-\infty}^{\infty} \int_{-\infty}^{\infty} \mathcal{W}_{ff^*} \left( -\frac{f_0}{\kappa} \left[ \boldsymbol{\Omega} + \frac{\omega_0}{2} \right]; 0 \right) & \\ \times \mathcal{W}_{ff^*} \left( -\frac{f_0}{\kappa} \left[ \boldsymbol{\Omega} - \frac{\omega_0}{2} \right]; 0 \right) & \\ \times \exp(i\mathbf{r}_0 \boldsymbol{\Omega}) d\boldsymbol{\Omega}. & \end{aligned} \quad (25)$$

In the second cascade, the exact Fourier transform described by matrix (22) (the focal distances of both lenses are assumed to be equal) is held as well. Then the distribution of the diffracted amplitude on the output of the second cascade can be written as

$$\begin{aligned} \mathcal{W}_{gg^*}(\mathbf{r}_0; \omega_0) = & \\ \mathcal{W}_{|g_1|^2 |g_1|^2} \left( -\frac{f_0}{\kappa} \omega_0; \frac{\kappa}{f_0} \mathbf{r}_0 \right). & \end{aligned} \quad (26)$$

According to the similar restoration scheme on the output of the second cascade one finds the distribution of the intensity of correlation field, which with the help of (21) can be written as

$$\begin{aligned} |g(\mathbf{r})|^2 = & \left( \frac{1}{\lambda f_0} \right)^2 \left| \mathcal{W}_{f_1 f_1^*}(-\mathbf{r}; 0) \right. \\ & + \mathcal{W}_{f_2 f_2^*}(-\mathbf{r}; 0) + \mathcal{W}_{f_1 f_2^*}(-\mathbf{r}; 0) \\ & \left. + \mathcal{W}_{f_2 f_1^*}(-\mathbf{r}; 0) \right|^2. & \end{aligned} \quad (27)$$

Hence we have obtained an important result. Namely, the correlation field on the output of the JTC is described by the coordinate-frequency distribution of the input signal at the zero spatial frequency  $\omega_0 = \mathbf{0}$ . At the value of the transverse shift of phase elements  $b \geq 2NT$ , the components of the distribution in (27) do not overlap and the square of the sum transforms into the sum of the squares of the distribution. Two first distributions describe the autocorrelation field of the 0th order of diffraction from two phase elements independently on their positions. It is especially interesting to consider the cross-correlation field that is formed in the  $\pm 1$ st order of diffraction from the shift of two phase elements in the input of the JTC

$$|g^{(\pm 1)}(x, y)|^2 = \frac{1}{(2\pi)^2} \left( \frac{k_2}{f_0} \right)^2 \times \left| \mathcal{W}_{f_1 f_2^*}(-x, -y \pm 2b; 0, 0) \right|^2. \quad (28)$$

Let us write explicitly distribution (28). On the basis of definition (7) for  $\omega_0 = \mathbf{0}$  the distribution determines the correlation function of the optical signals

$$\mathcal{W}_{f_1 f_2^*}(x_0, y_0; 0, 0) = \varphi_{12}(x_0, y_0). \quad (29)$$

The autocorrelation function of the elementary cell (14) is given as a product of triangle pulses [14]

$$\mathcal{W}_{f_0 f_0^*}(x_0, y_0; 0, 0) = \varphi(x_0, y_0) = \text{tri} \left( \frac{x_0}{T_x} \right) \text{tri} \left( \frac{y_0}{T_y} \right). \quad (30)$$

As a result, one gets on the basis of formula (12) the cross-correlation function of two binary phase elements, as the expansion of triangle pulses:

$$\varphi_{12}(x_0, y_0) = \sum_{k=-(N-1)}^{N-1} \sum_{l=-(M-1)}^{M-1} Q_{kl}^{(1)} \times \text{tri} \left( \frac{x_0 - kT_x}{T_x} \right) \text{tri} \left( \frac{y_0 - lT_y}{T_y} \right). \quad (31)$$

In the present case the expansion coefficients  $Q_{kl}^{(1)}$  and  $Q_{kl}^{(2)}$  are calculated according to the formula (17)

$$Q_{kl}^{(1)} = \sum_{n=1}^{N-k} \sum_{m=1}^{M-l} A_{n+k} B_{m+l} B_{nm},$$

$$Q_{kl}^{(2)} = \sum_{n=1}^{N-k} \sum_{m=1}^{M-l} A_{n+k} B_{nm+l}. \quad (32)$$

They have the meaning of the discrete cross-correlation functions of the binary phase distribution of two phase elements with the matrices  $\mathbf{A}$  and  $\mathbf{B}$ . The presence of two types of correlation coefficients (32) can be explained by the fact that the coefficient  $Q_{kl}^{(1)}$  describes the cross-correlation of two phase elements in the plane in the direction of the I-III quadrants, whereas the coefficient  $Q_{kl}^{(2)}$  describes the cross-correlation of two phase elements in the plane in the direction of the II-IV quadrants.

### 3.2. Hadamard-Schur multiplication in the $4f_0$ scheme

Let us describe the  $4f_0$  scheme, consisting of the binary phase element  $f_A(x, y)$  with the matrix  $\mathbf{A} = [A_{nm}]$  in the input and the phase element  $f_B(x, y)$  with matrix  $\mathbf{B} = [B_{nm}]$  on the output (Fig. 3). We assume that the coordinate-frequency distribution  $\mathcal{W}_{f_A f_A^*}(\mathbf{r}_0; \omega_0)$ ,  $\mathcal{W}_{f_B f_B^*}(\mathbf{r}_0; \omega_0)$  are constructed for the given elements.

As a result of the first and the second Fourier transforms, the transformation of the conjugated coordinates of the distribution of the first elements are described by the product of the matrices like (22)

$$\mathbf{M}_{4f_0} = \begin{bmatrix} -1 & 0 \\ 0 & -1 \end{bmatrix}. \quad (33)$$

Then the diffracted amplitude  $g_1(x, y)$ , that is formed by the first phase element on the output of the  $4f_0$  scheme, in the input of the second phase element is described by the coordinate-frequency distribution

$$\mathcal{W}_{g_1 g_1^*}(\mathbf{r}_0; \omega_0) = \mathcal{W}_{f_A f_A^*}(-\mathbf{r}_0; -\omega_0). \quad (34)$$

Bearing this in mind it is worth to define the inverse phase element  $f_A^{\text{inv}}(x, y) = f_A(-x, -y)$  which is formed on the output of the  $4f_0$  scheme and is described by the matrix  $\mathbf{A}^{\text{inv}} = [A_{N+1-n, M+1-m}]$  according to the definition (2). It is easy to show that the

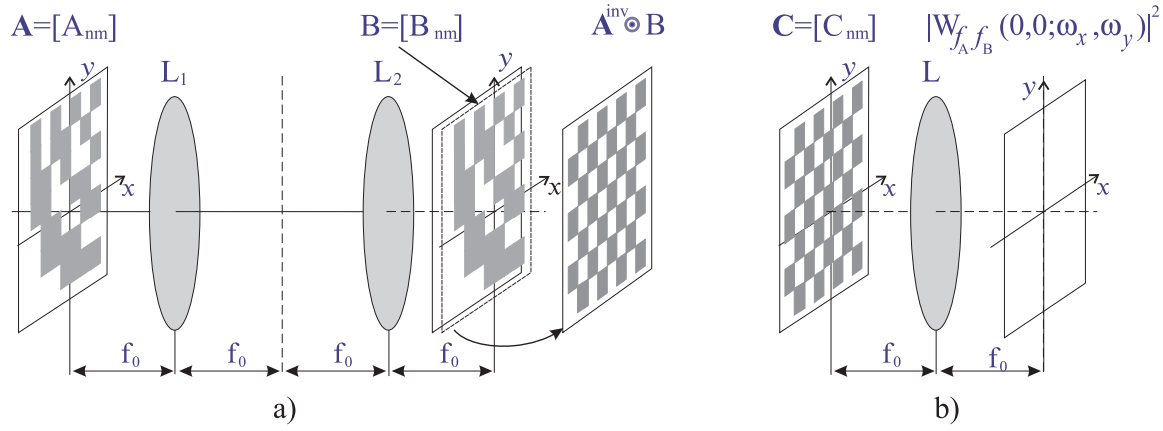


**Fig. 3.** Optical scheme which realizes the Hadamard-Schur multiplication of two phase elements  $\mathbf{A}^{\text{inv}}$  i  $\mathbf{B}$  (a) and the Fourier transformation of the element of the result of Hadamard multiplication  $\mathbf{C}$  (b).

Fourier spectrum of the inverse phase element is given by the complex conjugate function  $F^*(\omega_x, \omega_y)$ .

The presence of the second phase element on the output of the  $4f_0$  scheme corresponds to the optical realization of the *Hadamard-Schur multiplication* [25] of the inverse first phase element by the second phase element

$$\mathbf{C} = \mathbf{A}^{\text{inv}} \odot \mathbf{B} = [A_{N+1-n} \ M_{+1-m} \ B_{nm}]. \quad (35)$$

As a result one gets the new phase element  $\mathbf{C}$ .

Such a multiplication is described by a convolution with respect to the spatial frequency  $\omega_0$  of the distribution of two binary phase elements

$$\begin{aligned} \mathcal{W}_{f_C f_C^*}(\mathbf{r}_0; \omega_0) = \\ \mathcal{W}_{f_A f_A^*}(-\mathbf{r}_0; -\omega_0) \otimes_{\omega_0} \mathcal{W}_{f_B f_B^*}(\mathbf{r}_0; \omega_0). \end{aligned} \quad (36)$$

Let us add to the  $4f_0$  scheme the  $2f_0$  cascade in which the exact Fourier transform of the result of the Hadamard multiplication takes place. Such a cascade is described by the matrix (22) and in accordance with (23) the distribution of the diffracted amplitude

$$\mathcal{W}_{gg^*}(\mathbf{r}_0; \omega_0) = \mathcal{W}_{f_C f_C^*} \left( -\frac{f_0}{\kappa} \omega_0; \frac{\kappa}{f_0} \mathbf{r}_0 \right) \quad (37)$$

can be written through the coordinate-frequency distribution of the element, which is the result of the Hadamard multiplication.

On the basis of (36) the intensity of the diffracted light on the output plane of the  $2f_0$

cascade is the following

$$\begin{aligned} |g(\mathbf{r})|^2 = \frac{1}{(2\pi)^2} \int_{-\infty}^{\infty} \int_{-\infty}^{\infty} \mathcal{W}_{f_A f_A^*} \left( \frac{f_0}{\kappa} \omega_0; -\boldsymbol{\Omega} \right) \\ \times \mathcal{W}_{f_B f_B^*} \left( -\frac{f_0}{\kappa} \omega_0; -\boldsymbol{\Omega} \right) \exp(i\omega_0 \mathbf{r}) d\boldsymbol{\Omega} d\omega_0. \end{aligned} \quad (38)$$

If the integrand distribution of the binary phase elements are taken in the frequency representation (8), the two-fold integral can be done with the result

$$|g(\mathbf{r})|^2 = \left| \mathcal{W}_{F_A F_B} \left( \frac{\kappa}{f_0} \mathbf{r}; 0 \right) \right|^2. \quad (39)$$

Thus, one comes to the conclusion that the Wiener spectrum of spatial frequencies for the element of the Hadamard multiplication is described by the mutual coordinate-frequency distribution of two phase elements at the zero coordinate  $\mathbf{r}_0 = \mathbf{0}$ . In this case for the definition (8) in the frequency plane, the coordinate-frequency distribution yields the autocorrelation function of the Fourier spectrum of two signals. On the basis of formula (12) and taking into account formula (14) for the distribution of the shifted cells one gets

$$\begin{aligned} \mathcal{W}_{F_0 F_0^*}(\omega_{0x}; kT_x) = \\ \begin{cases} \text{sinc}(\omega_{0x} T_x / 2\pi); & \text{for } k = 0; \\ 0; & \text{for } k \neq 0. \end{cases} \end{aligned} \quad (40)$$

The similar expression is valid for the distribution  $\mathcal{W}_{F_0 F_0^*}(\omega_{0y}; lT_y)$ . In such case the external sums with respect to  $k$  and  $l$  reduce to

one term

$$\begin{aligned}
 Q_{00}^{(1)}(\omega_{0x}, \omega_{0y}) &\equiv \\
 Q_{00}^{(2)}(\omega_{0x}, \omega_{0y}) &= \sum_{n=1}^N \sum_{m=1}^M A_{nm}^{inv} B_{nm} \\
 &\times \exp \{-i[nT_x \omega_x + mT_y \omega_y]\}. \quad (41)
 \end{aligned}$$

According to the definition (13) the sums with respect  $n$  and  $m$  mean that there is an element by element multiplication of two elementary cells of phase elements, i.e. the multiplication (35) is realized.

As a result, for the coordinate-frequency distribution of the new phase element  $\mathbf{C}$  one gets the following expression

$$\begin{aligned}
 \mathcal{W}_{FF^*}(\omega_{0x}, \omega_{0y}; 0, 0) &= C_{NM}(\omega_{0x}, \omega_{0y}) \\
 &\times Q_{00}^{(1)}(\omega_{0x}, \omega_{0y}) \mathcal{W}_{F_0 F_0^*}(\omega_{0x}, \omega_{0y}; 0, 0), \quad (42)
 \end{aligned}$$

that is equivalent to the Fourier spectrum (4) of the component elements.

Comparing (27) and (39) one notes that particular cases of coordinate-frequency distribution are realized in the optical schemes.

#### 4. Classes of the binary phase elements

The statistical description of the binary phase elements is based on the matrix  $\mathbf{S}$  of the scalar products of the rows (or columns) of the matrix  $\mathbf{A}$

$$\mathbf{S}^r = \mathbf{A}\mathbf{A}', \quad \mathbf{S}^c = \mathbf{A}'\mathbf{A}. \quad (43)$$

We shall study statistical distribution of the off-diagonal elements of this matrix

$$p(s) = \frac{1}{N(N-1)} \sum_{i \neq j} \delta_{s-S_{ij}, 0}. \quad (44)$$

Further it will be shown that the second moment of this distribution

$$d_A = \sum_{s=-N}^N s^2 p(s) = \frac{1}{N(N-1)} \sum_{i \neq j} S_{ij}^2, \quad (45)$$

which we call the non-orthogonality parameter, allows to classify partially an essential part of all possible binary phase elements. Let us note that the distribution (44) (and therefore all its moments) does not depend on a

permutation of the rows (columns) of the matrix  $\mathbf{A}$ . Besides, even moments do not depend on the change of the sign of separate rows (columns).

The introduced in this Section classification concerns an essential part of the set of the binary phase elements however does not exhaust that set. It deals with orthogonal and collinear BPE (ordered) and the random BPE into which all BPE transform after complete randomization.

#### 4.1. Orthogonal BPE

The orthogonal BPE (Fig. 1 (a)) are given by the Hadamard matrices  $\mathbf{H}$ , that are a subset of the orthogonal matrices. The description of the Hadamard matrices and the ways to construct them can be found in [10–12]. A general algorithm of the construction of the Hadamard matrices of higher orders is based on the usage of the direct (Kronecker) product [15] of two Hadamard matrices  $\mathbf{H}_N, \mathbf{H}_M$  having arbitrary sizes  $N$  and  $M$

$$\mathbf{H}_{MN} = \mathbf{H}_N \times \mathbf{H}_M. \quad (46)$$

As a result, one gets the Hadamard matrix of the size  $NM$ .

It is worth to separate two typical non-normalized Hadamard matrices of 4th order which will be studied in what follows

$$\begin{aligned}
 \mathbf{H}_4^{(s)} &= \begin{bmatrix} -1 & 1 & -1 & -1 \\ -1 & 1 & 1 & 1 \\ 1 & 1 & 1 & -1 \\ -1 & -1 & 1 & -1 \end{bmatrix}, \\
 \mathbf{H}_4^{(d)} &= \begin{bmatrix} -1 & 1 & 1 & 1 \\ 1 & -1 & 1 & 1 \\ 1 & 1 & -1 & 1 \\ 1 & 1 & 1 & -1 \end{bmatrix}.
 \end{aligned}$$

The matrix  $\mathbf{H}_4^{(s)}$  is characterized by parameter  $r = 0$  i.e.  $\mathcal{N}_+ = \mathcal{N}_-$ , and it has  $S$ -like structure. The matrix  $\mathbf{H}_4^{(d)}$ , is characterized by the maximal value of the parameter  $r$  (in the present case  $r = 2$ ) and it has a typical "diagonal structure".

Due to the orthogonality of the matrices  $\mathbf{H}$  the matrices from the scalar products of their rows (or columns) are diagonal

$$\mathbf{S} = \mathbf{H}\mathbf{H}' = N\mathbf{I}, \quad (47)$$

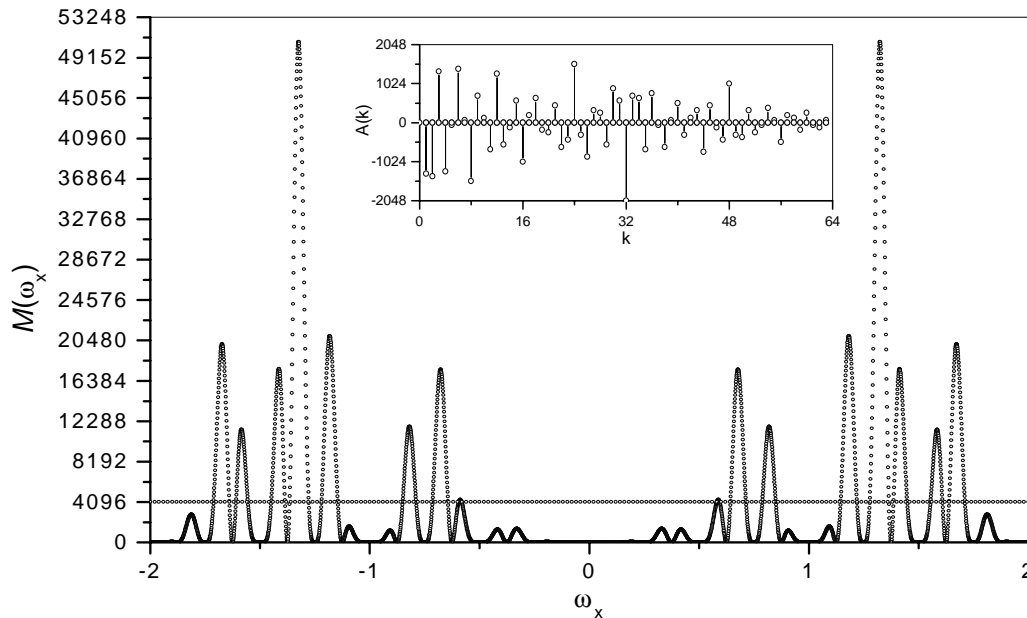


**Fig. 4.** Wiener spectrum of the orthogonal phase elements 1) - the canonical Hadamard matrix; 2) -  $S$ -like (non-normalized) Hadamard matrix.

where  $N$  is the size  $\mathbf{H}$  and the distribution of its off-diagonal elements (44) has the form of the single peak located at the zero

$$p(s) = \delta_{s,0}. \quad (48)$$

Evidently, their non-orthogonality parameters are equal to zero  $d_A = 0$ .

Let us further analyse their optical properties. For the class of orthogonal phase elements the correlation coefficients  $Q_{k0}^{(1)} = Q_{0l}^{(1)} \equiv 0$ .

We shall restrict ourselves to the analysis of the one-dimensional modulation function for the class of the orthogonal phase elements. From formula (16) the modulating function becomes simpler in the direction of orthogonality (e.g. along  $\omega_x$  axis) [28]

$$\begin{aligned} \mathcal{M}(\omega_x, 0) &= NM \\ &+ 2 \sum_{k=1}^{N-1} \left[ \sum_{l=1}^{M-1} Q_{kl}^{(1)} + Q_{kl}^{(2)} \right] \cos \omega_x k T_x. \end{aligned} \quad (49)$$

From this formula one can see that for different types of orthogonal phase elements since  $Q_{kl}^{(1)} \neq 0$  and  $Q_{kl}^{(2)} \neq 0$  the Wiener spectrum of the phase element (15) is formed as a result of modulation of the Wiener spectrum of the elementary cell  $|F_0(\omega_x)|^2$  by the periodic modulation function (49).

For the class of normalized orthogonal phase elements the function (49) has its peculiarities. At an arbitrary chosen sequence of rows (columns) of the elementary cells of phase elements the following relations for the correlation coefficients are held

$$\begin{aligned} A(l) &= \sum_{k=1}^{N-1} [Q_{kl}^{(1)} + Q_{kl}^{(2)}] \equiv 0; \\ A(k) &= \sum_{l=1}^{M-1} [Q_{kl}^{(1)} + Q_{kl}^{(2)}] \equiv 0, \end{aligned} \quad (50)$$

i.e. in the orthogonality direction the Wiener spectrum of the class of orthogonal phase elements reduces to the spectrum of elementary cell. This is a general property of all normalized Hadamard matrices.

In Fig. 4 we have depicted the modulation function (49) of Wiener spectrum and the corresponding coefficients (50) of the orthogonal phase elements.

It should be stressed that for the phase element, which is described by the canonical Hadamard matrix  $\mathcal{M}(\omega_x, 0) = \text{const}$ . Numerical calculations show that  $k$  and  $l$   $Q_{kl}^{(1)} = -Q_{kl}^{(2)}$  for all  $k$  and  $l$ . Thus the relation (50) are satisfied automatically.

As one can see from Fig. 4, in general case of non-normalized Hadamard matrices

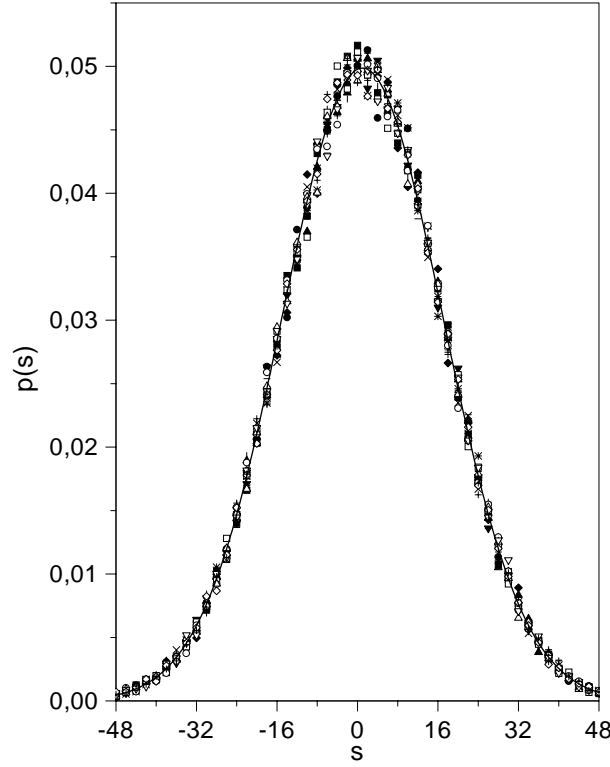


**Fig. 5.** The distribution of the off-diagonal elements of the matrices  $\mathbf{S}$  for 16 random matrices.

the correlation coefficients  $A(k) \neq 0$  and, thus, the relations (50) are not satisfied.

#### 4.2. Collinear BPE

The collinear BPE (Fig. 1 (c)) are described by the binary rectangle matrices composed from identical rows (columns) which differ only by signs. They can be written in the form of direct (Kronecker) product of two binary vectors  $\mathbf{X}$  та  $\mathbf{Y}$

$$\mathbf{C} = \mathbf{Y} \otimes \mathbf{X} = [Y_n X_m]. \quad (51)$$

If the size of the vector  $\mathbf{Y}$  is  $N$  and the size of the vector  $\mathbf{X}$  is  $M$  the corresponding distribution of the off-diagonal elements of the matrices composed from scalar products  $\mathbf{S}^r$  and  $\mathbf{S}^c$  will have the following form

$$\begin{aligned} p(s) &= P_-^r \delta_{s+M} + P_+^r \delta_{s-M}, \\ p(s) &= P_-^c \delta_{s+N} + P_+^c \delta_{s-N}. \end{aligned} \quad (52)$$

The heights of the peaks  $P_{\pm}^r$  and  $P_{\pm}^c$  depend on the ratio of positive and negative elements of vectors  $\mathbf{Y}$  and  $\mathbf{X}$ , respectively.

Formally one can get that the parameter  $d_A = M^2$  for matrix  $\mathbf{S}^r$  and  $d_A = N^2$  for the

matrix  $\mathbf{S}^c$ . Evidently, it has the meaning of the non-orthogonality parameter only for the square matrices when  $N = M$ .

For the class of collinear elements the correlation coefficients (17) become simpler

$$Q_{kl}^{(1)} = Q_{kl}^{(2)} = Q_k^{(x)} Q_l^{(y)}, \quad (53)$$

where the discrete correlation functions of the basic row and column are defined as

$$\begin{aligned} Q_k^{(x)} &= \sum_{n=1}^{N-k} X_{n+k} X_n; \\ Q_l^{(y)} &= \sum_{m=1}^{M-l} Y_{m+l} Y_m. \end{aligned} \quad (54)$$

Correspondingly the modulation function can be written as a product

$$\mathcal{M}(\omega_x, \omega_y) = \mathcal{M}(\omega_x) \mathcal{M}(\omega_y). \quad (55)$$

of two one-dimensional periodic functions in the form of Fourier series with correlation coefficients (54)

$$\begin{aligned} \mathcal{M}(\omega_x) &= N + 2 \sum_{k=1}^{N-1} Q_k^{(x)} \cos \omega_x k T_x; \\ \mathcal{M}(\omega_y) &= M + 2 \sum_{l=1}^{M-1} Q_l^{(y)} \cos \omega_y l T_y. \end{aligned} \quad (56)$$

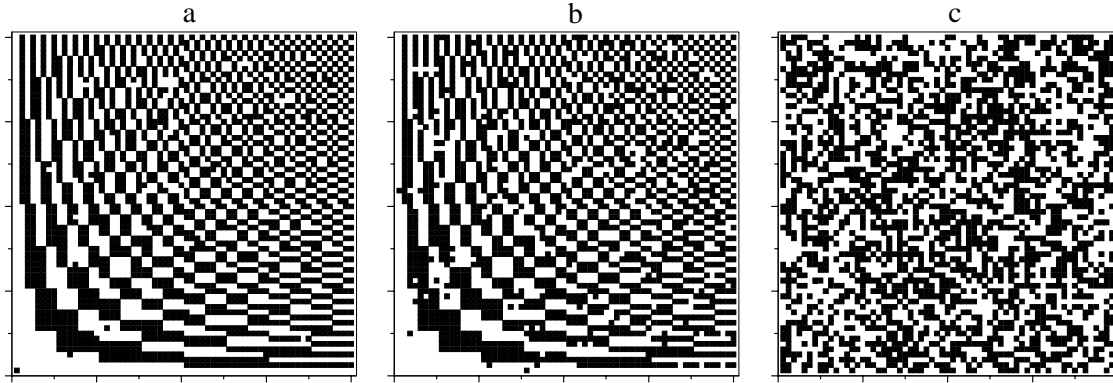


**Fig. 6.** Binary phase elements obtained as a result of randomization of the structure shown in fig. 1 a: after  $k = 16$  (a) ( $d_A \approx 4$ ),  $k = 70$  (b) ( $d_A \approx 16$ ),  $k = 2000$  (c) ( $d_A \approx 64$ ) steps of randomization.

Function  $\mathcal{M}(\omega_x)$  is equal to zero at  $\omega_x = 0$ . If the basic row  $X_n$  and the basic column  $Y_m$  has  $N/2$  and  $M/2$  elements equal to  $-1$ , respectively, (54) the following relation is valid for the correlation coefficients

$$\begin{aligned} N + 2 \sum_{k=1}^{N-1} Q_k^{(x)} &= 0; \\ M + 2 \sum_{l=1}^{M-1} Q_l^{(y)} &= 0. \end{aligned} \quad (57)$$

By numerical calculations we found that a number of changes of the sign for the correlation coefficients  $Q_k^{(x)}$  and  $Q_l^{(y)}$  are equal to a number of changes of the sign for the basic vectors  $X_n, Y_m$ .

### 4.3. Random BPE

Historically, the random BPE were the first BPE used in optical systems for image recognition (Fig. 1 (b)) [1–3]. The matrix elements that correspond to this BPE take the values  $\pm 1$  with certain probability. We shall unify into the equivalent subsets the square matrices of the same size  $N$  with the same ratio of the positive  $\mathcal{N}_+$  and negative  $\mathcal{N}_-$  elements. Evidently, the scalar products of their rows (columns) have random values in the interval  $-N \dots + N$ . In the paper [13] it was shown that their distribution (44) is the Gaussian one

$$p(s) = \frac{2}{\sqrt{2\pi\sigma^2}} e^{-\frac{(s - \langle s \rangle)^2}{2\sigma^2}},$$

$$\langle s \rangle = \frac{r^2}{N}, \quad \sigma^2 = N \left( 1 - \frac{r^4}{N^4} \right). \quad (58)$$

The parameter  $r = (\mathcal{N}_+ - \mathcal{N}_-) / N$  describes the relation of positive and negative elements of the matrix  $\mathbf{A}$ .

In Fig. 5 we display the results of a numerical computation for sixteen random matrices having the size  $N = 256$ . The solid curve corresponds to computation according to the analytical expression (58).

The non-orthogonality parameter for random matrices is equal to

$$d_A = \sigma^2 + \langle s \rangle^2 = N \left( 1 + \frac{r^4}{N^3} - \frac{r^4}{N^4} \right). \quad (59)$$

Evidently, these are the mean values for a subset of all random matrices of size  $N$  with the parameter  $r$ . The parameters  $\langle s \rangle$  and  $\sigma^2$  as well as  $d_A$  for any concrete matrix differ from the mean values because of fluctuations.

### 4.4. Randomization of the ordered phase elements

The binary matrices with the intermediate values of the non-orthogonality parameter may be obtained from the ordered ones using randomization algorithm. Every step of this algorithm is the following: random coordinates of two elements of the matrix  $\mathbf{A}$  are generated and, if the elements are different we permute them. A usage of this algorithm leads to increase the non-orthogonality parameter

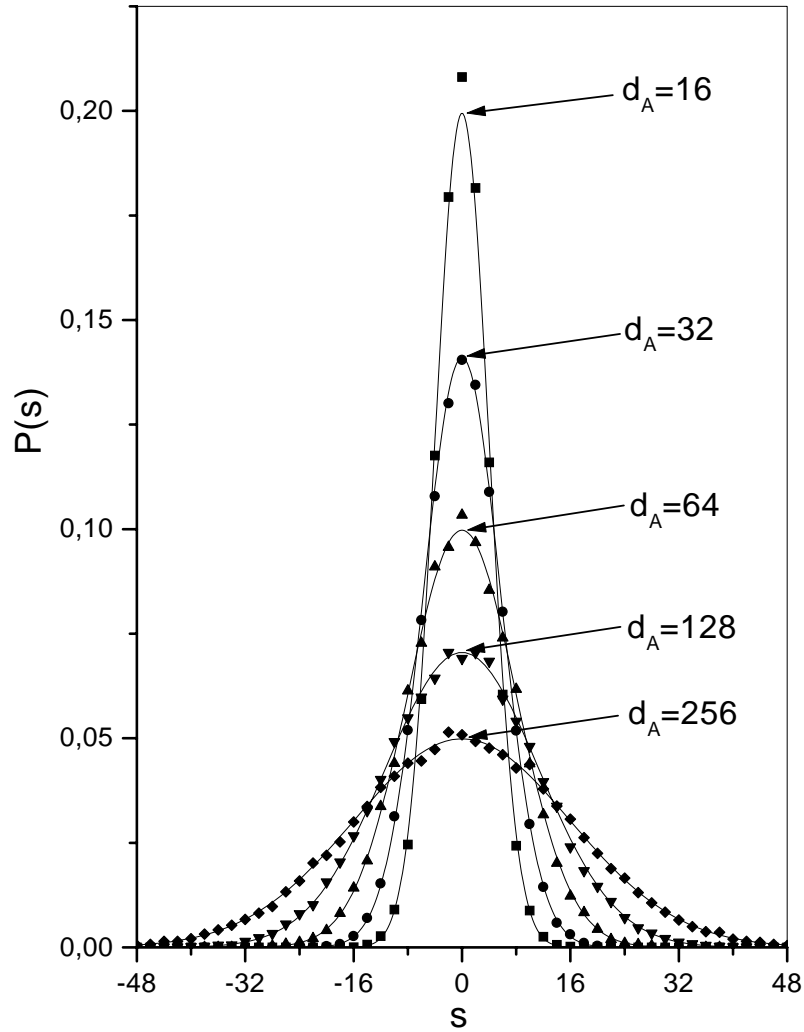


**Fig. 7.** Distribution  $p(s)$  of the off-diagonal elements of the matrix  $S$  for different values of the non-orthogonality parameter  $d_A$  for randomization of the orthogonal matrix having size  $N = 256$ .

for the orthogonal matrices and to decrease this parameter for the collinear matrices.

After a sufficiently large number of randomization steps  $k$  all matrices become random and further randomization does not turn out from this class. Such a saturation is connected with the fact that the randomization algorithm permutes any two different elements including those being permuted. Let us note, that the value of  $r$  conserves under such process. Besides, the obtained matrices during a sufficiently large number of steps "remember" their initial structure and "forget" it only after entering into the random region. From the physical point of view this means that the phase mask contains large connected clusters of the initial structure, sizes of which

decrease while the non-orthogonality parameter tends to the value approximately equal to  $N$ .

#### 4.5. Quasi-orthogonal BPE

An application of the randomization algorithm to the orthogonal BPE permits one to construct a class of quasi-orthogonal BPE that is an intermediate one between the orthogonal and random BPE.

The described algorithm is illustrated in Fig. 6, where we show three masks obtained from the mask described by the canonical Hadamard matrix (Fig. 1 (a)) after  $k = 16$  (a),  $k = 70$  (b),  $k = 2000$  (c) steps of randomization.

Numerical calculations show (Fig. 7) that the randomized orthogonal matrices have the distribution (44) which is rather exactly described by (58). In the paper [13] the analytical dependences of the parameters  $\langle s \rangle$  and  $\sigma^2$  on the number of randomization steps  $k$  and the number of permuted elements  $\mathcal{N}_{ch}$  were found. Using these results and (58) we have obtained the solid lines in Fig. 7. In Ref. [13] the similar dependences for the non-orthogonality parameter were found. It was shown that this parameter increased during randomization from  $d_A = 0$  to  $d_A \approx N$ .

Early it is shown that for the class of normalized orthogonal phase elements one has  $\mathcal{M}(\omega_x, 0) \equiv NM$ . Let us examine the properties of that function during reorthogonalization.

In Fig. 8 the modulation function  $\mathcal{M}(\omega_x, 0)$  of the Wiener spectrum for three different quasi-orthogonal phase elements obtained as a result of randomization of the canonical Hadamard matrix are shown.

This Figure shows that if  $d_A = 4$ , the obtained matrix (Fig. 6 (a)) visually almost not differ from the canonical Hadamard matrix (Fig. 1 (a)), the majority of the correlation coefficients  $A(k) \neq 0$  and the modulation function  $\mathcal{M}(\omega_x, 0)$  respectively is characterized by more complicated dependence, in which a series of local maxima (minima) appears. With the increase of  $d_A$  one observes an increase of the intensity of modulation function fluctuations, the maximal value of which corresponds to the region of random phase elements with  $d_A \approx N$ . One can state that the formation of a fine structure of local maxima/minima has purely random character since we only analyse the frequency axis  $\omega_x$  and during the randomization the change of the cell position takes place in all plane of phase element.

#### 4.6. Quasi-collinear BPE

Similarly to the quasi-orthogonal BPE by means of the randomization of the collinear BPE one can construct the class of the quasi-collinear BPE (Fig. 9)

In the paper [28] it is shown that the distribution (44) for quasi-collinear matrices, which are obtained from the collinear one of

the "chess-like" structure (Fig. 1(c)), is given by

$$p(s) = \frac{1}{\sqrt{2\pi\sigma^2}} \times \left\{ \left( 1 + \frac{1}{N-1} \right) \exp \left( -\frac{(s + \langle s \rangle)^2}{2\sigma^2} \right) + \left( 1 - \frac{1}{N-1} \right) \exp \left( -\frac{(s - \langle s \rangle)^2}{2\sigma^2} \right) \right\}. \quad (60)$$

The dependences of  $\langle s \rangle$  and  $\sigma^2$  on the step of randomization  $k$  and the number of permuted elements  $\mathcal{N}_{ch}$  are also found in this paper.

In Fig. 10 we show by symbols the distribution of the collinear matrix (like chess board) of the size  $N = 256$  after certain steps of randomization found numerically. Solid curves depicted the analytical dependences (60) with parameters were calculated according to the corresponding formulae [28].

### 5. The generalized optical parameter

In the present Section we shall introduce the generalized optical parameter on the basis of the results of the study of the Wiener spectra properties and correlation field for the binary phase elements.

In the previous paper [13] it was suggested to introduce the generalized optical parameter to characterize a fine structure of the Wiener spectra interference maxima (minima).

To estimate the fine structure let us introduce the difference function

$$\Delta(\omega_x, \omega_y) = [\mathcal{M}(\omega_x, \omega_y) - NM] \times |F_0(\omega_x)F_0(\omega_y)|^2, \quad (61)$$

that describes the deviation of the Wiener spectrum intensity in the frequency plane for the phase element from that quantity for the elementary cell.

The difference function (61) may take both positive and negative values. To characterize fluctuations it is important to consider the value of the difference function rather than its sign. Therefore, let us construct the normalized function and let us perform its averaging with respect to all spatial frequencies

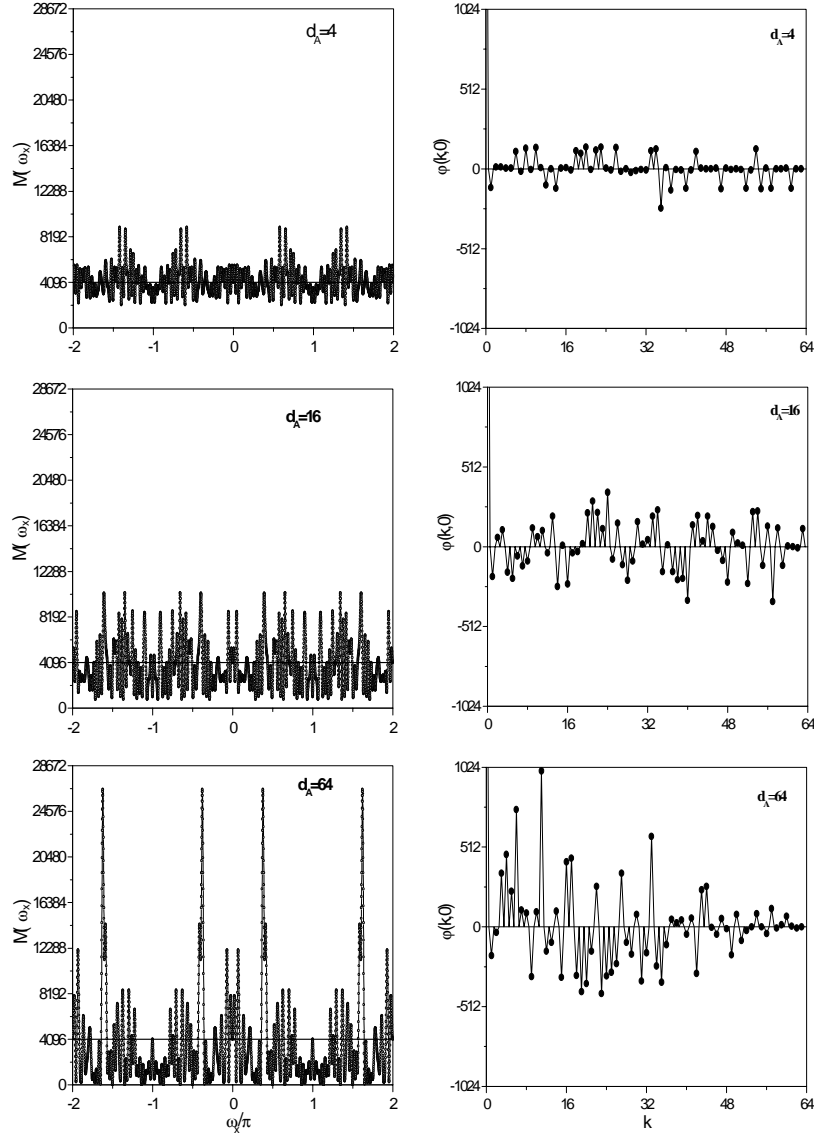


**Fig. 8.** Modulation functions  $\mathcal{M}(\omega_x, 0)$  of the Wiener spectra and the corresponding discrete autocorrelation function  $A(k)$  quasi-orthogonal phase elements depicted in Fig. 6.

in the 0th and  $\pm 1$ st orders of diffraction

$$\langle |\Delta(\omega_x, \omega_y)|^2 \rangle = \frac{1}{(2\pi)^2} \int_{-\pi/T_x}^{\pi/T_x} \int_{-\pi/T_y}^{\pi/T_y} |\mathcal{M}(\omega_x, \omega_y) - NM|^2 d\omega_x d\omega_y. \quad (62)$$

On the basis of (16) the integration with respect to  $d\omega_x$  or  $d\omega_y$  reduces to  $1/2 [\text{sinc}(k - k') + \text{sinc}(k + k')]$ . As a result one gets important relation

$$\langle |\Delta(\omega_x, \omega_y)|^2 \rangle = \frac{2}{N^2 M^2} \left\{ \sum_{k=1}^{N-1} Q_{k0}^{(1)2} + \sum_{l=1}^{M-1} Q_{0l}^{(1)2} + \sum_{k=1}^{N-1} \sum_{l=1}^{M-1} [Q_{kl}^{(1)2} + Q_{kl}^{(2)2}] \right\}. \quad (63)$$

This relation will be taken as a definition of the generalized optical parameter, which is determined only by the binary phase distribution. Such parameter characterizes the averaged level of the intensity of fluctuations of the Wiener spectrum of the phase element. The statistical analysis of the numerical results show that in spite of essential fluctuations the increase of the value of optical parameter  $\langle |\Delta(\omega_x, \omega_y)|^2 \rangle$ , as a function of the non-orthogonality parameter  $d_A$  is a linear function [13].

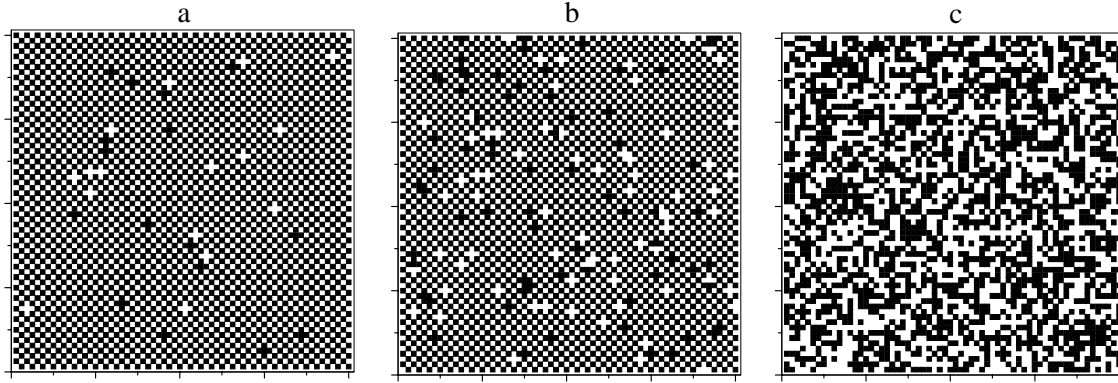


**Fig. 9.** Binary phase elements obtained as a result of randomization of the structure shown in Fig. 1 c: after  $k = 16$  (a) ( $d_A \approx 3850$ );  $k = 70$  (b) ( $d_A \approx 3118$ );  $k = 2000$  (c) ( $d_A \approx 68$ ) steps of randomization.

### 5.1. Optical noise level

According to (29) the coordinate-frequency distribution uniquely defines the autocorrelation function  $\varphi(x_0, y_0)$  of the phase element. For an arbitrary binary phase distribution at  $x_0 = y_0 = 0$  one has a global maximum of the intensity of the autocorrelation function

$$|\varphi(0, 0)|^2 = Q_{00}^{(1)2} = (NM)^4. \quad (64)$$

Then the quantity averaged with the respect to all cells of the phase element

$$\begin{aligned} \langle |\varphi(k, l)|^2 \rangle &= \frac{1}{N(M-1) + M(N-1)} \\ &\times \left\{ \sum_{k=1}^{N-1} Q_{k0}^{(1)2} + \sum_{l=1}^{M-1} Q_{0l}^{(1)2} \right. \\ &\left. + \sum_{k=1}^{N-1} \sum_{l=1}^{M-1} [Q_{kl}^{(1)2} + Q_{kl}^{(2)2}] \right\} \quad (65) \end{aligned}$$

characterizes the averaged value of the optical noise intensity, which is also determined by the binary phase distribution. Comparing with Eq. (63) one finds

$$\begin{aligned} \langle |\varphi(k, l)|^2 \rangle &= \frac{NM}{2[2 - (1/N + 1/M)]} \\ &\times \langle |\Delta(\omega_x, \omega_y)|^2 \rangle. \quad (66) \end{aligned}$$

Hence, the introduced generalized optical parameter with the accuracy up to constant multiplier characterizes the level of the optical noise of the binary phase element.

We may determine signal-to-noise ratio (**SNR**) of the binary phase element as follows

$$\text{SNR} = \frac{(NM)^2}{\langle |\varphi(k, l)|^2 \rangle}. \quad (67)$$

This quantity is an important characteristic of the binary phase element for holographic systems of the image recognition.

## 6. Two-parametric representation

### 6.1. Relation between the classes of the orthogonal and collinear phase elements

The Hadamard-Schur product of the canonical Hadamard matrix  $\mathbf{H}_{can}$  by the inverse one  $\mathbf{H}_{can}^{inv}$  (see Fig. 1 (a)) gives a periodic collinear matrix  $\mathbf{P}$  of the chess-like structure (Fig. 1 (c)).

$$\mathbf{H}_{can} \circ \mathbf{H}_{can}^{inv} = \mathbf{C}. \quad (68)$$

One can easily see that an arbitrary matrix  $\mathbf{H}$ , an arbitrary collinear matrix  $\mathbf{C}$ , their Hadamard-Schur product  $\mathbf{H} \odot \mathbf{C}$ , and matrix  $\mathbf{O}$ , all elements of which equal to unity form a group with the respect to the Hadamard-Schur multiplication. Evidently, all of them are square and of the same size.

The product like (68) may be generalized for an arbitrary quasi-orthogonal matrix  $\mathbf{A}$ , obtained as a result of randomization of the canonical Hadamard matrix  $\mathbf{H}_{can}$ .

We have found [28], that knowing the non-orthogonality parameter of the matrix  $\mathbf{A}$ ,

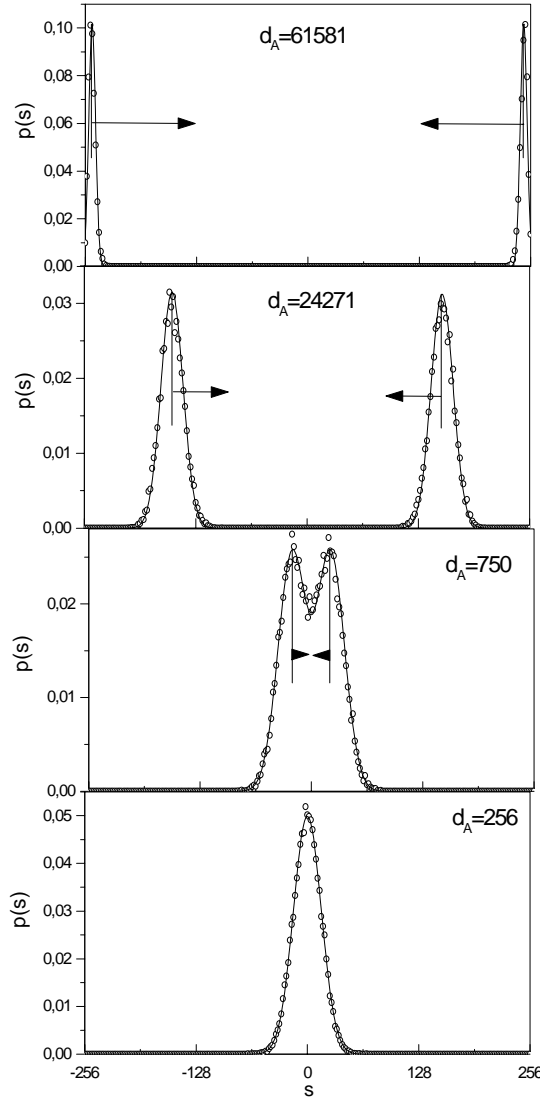


**Fig. 10.** Evolution of the distribution of the off-diagonal elements of the matrix  $\mathbf{S}$  while randomizing the collinear matrix of the size  $N = 256$ .

one can find uniquely the non-orthogonality parameter of the resulting matrix of the Hadamard multiplication  $\mathbf{C}$  (68) as follows

$$\mathbf{C}^{(1)} = \mathbf{A} \circ \mathbf{H}_{can}^{inv} \implies d_{C^{(1)}} = N + N(N-1) \left(1 - \frac{d_A}{N}\right); \quad (69)$$

$$\mathbf{C}^{(2)} = \mathbf{A} \circ \mathbf{A}^{inv} \implies d_{C^{(2)}} = N + N(N-1) \left(1 - \frac{d_A}{N}\right)^2. \quad (70)$$

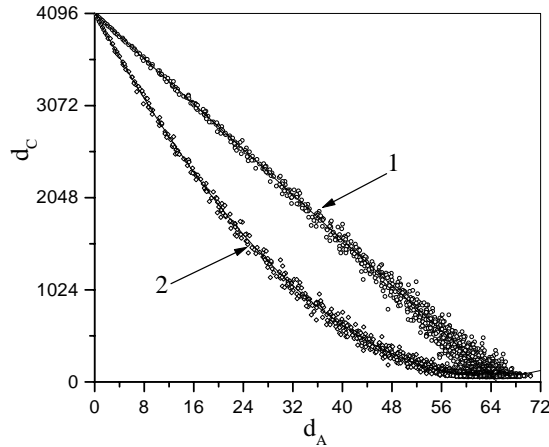
It should be noted that similarly to (68) in both cases the matrices  $\mathbf{C}^{(1)}$  and  $\mathbf{C}^{(2)}$  belong to the class of quasi-collinear matrices.

Fig. 11 illustrates the dependences (69), (70) (solid curves) in comparison with the re-

sults of the direct numerical calculations of the parameter  $d_C$ .

Direct numerical calculations confirm the linear (69) and parabolic (70) dependences of the non-orthogonality parameter of the resulting matrix of the Hadamard multiplication  $\mathbf{C}$ . The obtained results show that there is a relationship between the introduced above classes of quasi-orthogonal and quasi-collinear phase elements.

Let us stress that the construction of the matrices with the intermediate values of the non-orthogonality parameter by means of randomization does not exhaust all set of matrices with the given parameter  $d_A$ , since it is possible to construct the matrices with the



**Fig. 11.** Linear (1) and parabolic (2) dependences between the non-orthogonality parameter  $d_A$  of the quasi-orthogonal and quasi-collinear matrices.

same  $d_A$  but with the distributions different from (48) or (52).

## 6.2. Two-parameter representation of the properties of the different classes of the BPE

In Fig. 12 we have depicted the dependences of the optical noise level  $\langle |\varphi(k, l)|^2 \rangle$  of different classes of the BPE of the size  $64 \times 64$  on the value of the parameter  $d_A$  (in log – log scale) [31].

From Fig. 12 one can see that all curves meet each other in region III of random matrices while performing randomization of both the orthogonal and collinear matrices. Note that all dependences  $\langle |\varphi(k, l)|^2 \rangle$  on the non-orthogonality parameter  $d_A$  are linear in average. This means that independently on the way of generation of the random phase elements all the ensemble of possible values of  $\langle |\varphi(k, l)|^2 \rangle$  and  $d_A$  does not leave the bounded (usually ellipsoidal) region III.

Curves 1 and 5 are the boundary curves for the given two-parameter representation. The canonical Hadamard matrix (including region II of the quasi-orthogonal matrices) has larger **SNR** in comparison with the random matrices. On the contrary, the matrix with chess-like structure is characterized by the maximal value of the optical noise level.

Numerical computations show that there is a relation between the boundary curves 1 and 2. Independently of the algorithm of

element by element randomization the producing of the collinear matrices (region IV) may be considered as the result of Hadamard-Schur multiplication (69),(70) of the quasi-orthogonal matrices (region IV) produced from the canonical Hadamard matrix. It should be noted that after using initially the algorithm of randomization the rows/columns of the orthogonal matrix one finds that further element by element randomization does not lead to the change of the optical noise level (curve2). On the other hand, by means of the minimization of the parameter  $\langle |\varphi(k, l)|^2 \rangle$  (curve 7) for the collinear matrix one can reach optical noise level of the random matrices.

The initial values of the parameter  $\langle |\varphi(k, l)|^2 \rangle$  are as follows: 351.24 (curve 1) 981.875 (curve 2) 4004.83 (curve 3) 15814.3 (curve 4) 1893150 (curve 5) 473547 (curve 6) 1374.03 (curve 7). The averaged values of the optical noise  $\langle |\varphi(k, l)|^2 \rangle$  in the region of the random matrices for the matrices 1, 2, 3, 5, 6, 7 is equal to 1040 and for the matrix 4  $\langle |\varphi(k, l)|^2 \rangle$  is equal to 1502. Therefore, the ratio signal/noise for the matrices 1, 2, 3, 5, 6, 7 is 4.208 whereas for the matrix 4 it is 4.048. One should note that according to the definition (65) the value of the optical noise level  $\langle |\varphi(k, l)|^2 \rangle$  of the chess-like matrix is equal to the averaged value of the square of the "empty window" autocorrelation function. Then the value of  $\lg(1893150/1040) \approx 3.26$  characterizes the efficiency of the usage of the random

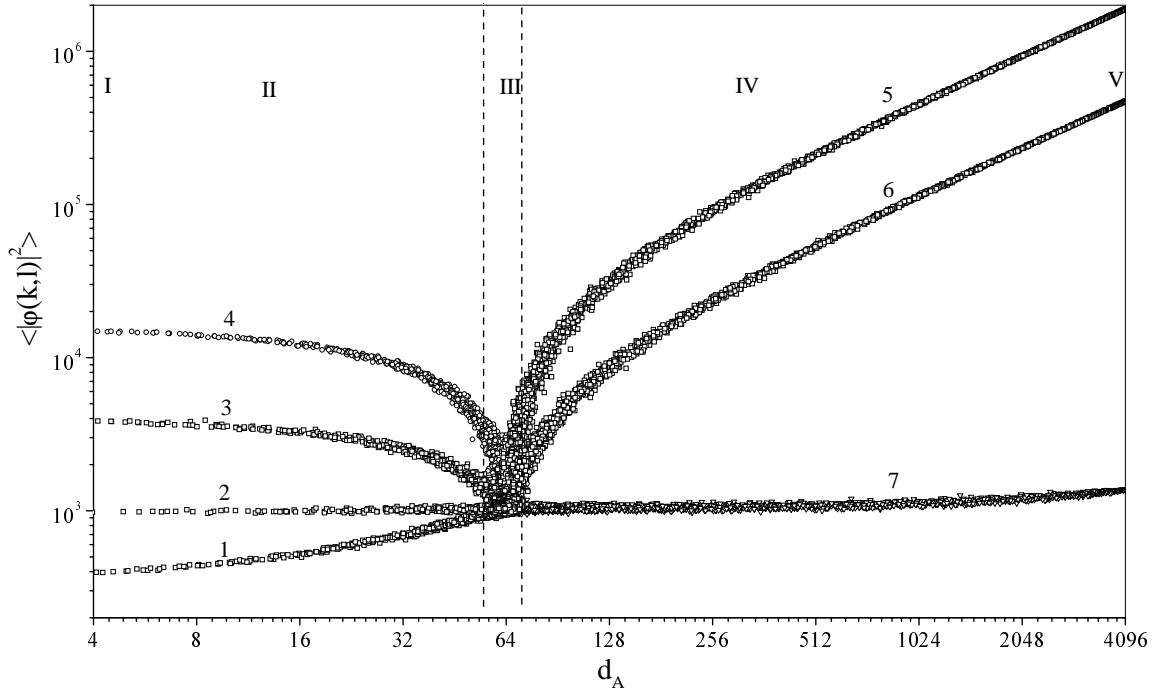


**Fig. 12.** The dependence of the optical noise level  $\langle |\varphi(k, l)|^2 \rangle$  on the non-orthogonality parameter  $d_A$  of different classes of the binary phase elements. Curves 1 - 4 describe randomization of the orthogonal phase elements of 1) the canonical Hadamard matrix; 2) the orthogonal matrix at  $r = 0$  with random positions of rows and columns; 3) and 4) the Kronecker degree 3 of the orthogonal matrices  $\mathbf{H}_4^s$  and  $\mathbf{H}_4^d$  respectively. Curves 5 - 7 describe randomization of the collinear phase elements of 5) and 6) the matrices of chess-like structure with the periods  $T$  and  $2T$  respectively; 7) the matrix, obtained as a result of minimization of the matrix 5 with respect to the parameter  $\langle |\varphi(k, l)|^2 \rangle$ .

binary phase elements for which the optical noise level decreases by more than three degrees.

The obtained results show that the two-parameter representation of the properties of the binary phase elements may be viewed as a kind of diagram representation.

## 7. Conclusions

On the basis of conducted researches is constructed coordinate-frequency distribution of the BFE. The technique of calculation of the Wigner spectrum of space frequencies of the BFE with usage of the modulation function  $\mathcal{M}(\omega_x, \omega_y)$  is circumscribed. By method of the signals distributions analytically description the optical schemes of correlation analysis and multiplying of the Hadamard - Schur of the two BFE. The parameter of a nonorthogonality  $d_A$  is offered, which numer-

ical values allow to class different types of the BFE. The boundary values  $d_A$  characterize:  $d_A = 0$  - class of orthogonal BFE;  $d_A = N^2$  - class of collinear BFE. Is placed, that for the class of random BFE  $d_A \approx N$ . The mechanism of generation of classes quasiothogonal ( $0 \leq d_A \leq N$ ) that quasicollinear ( $N \leq d_A \leq N^2$ ) BFE is circumscribed. For the characteristic of logical properties of different classes of the BFE the generalized optical parameter  $\langle |\varphi(k, l)|^2 \rangle$  is entered. The key possibility of the twoparameter of representation properties of the BFE is exhibited. On the basis of such representation the comparative analysis of the noise level of different classes of the BFE is conducted.

## Acknowledgments

The authors are grateful to Academician I.R.Yukhnovskii for permanent interest in this study and L. Muravsky, V. Fitio and P.Hlushak for fruitful discussions.

## References

1. Burckhardt C. B., *Appl. Opt.*, **9** (1970) 695.
2. Javidi B., Horner J. L., *Opt. Eng.* **33** (1994) 1752.
3. Fitio V., Muravsky L., Stefansky A., *Proc. SPIE*, **2747** (1995) 224.
4. Kallman R. R., Goldstein D. H., *Opt. Eng.*, **33** (1994) 1806.
5. Weaver C. S., Goodman J. W., *Appl. Opt.*, **5** (1966) 1248.
6. Takeda Y., Oshida Y., Miyamura Y., *Appl. Opt.*, **11** (1972) 818.
7. Nakayama Y., Kato M., *JOSA*, **69** (1979) 1367.
8. Walker S. J., Jahns J., *J. Opt. Soc. Am. A*, **7** (1990) 1509.
9. Gao G., Kostuk R., *Appl. Opt.*, **36** (1997) 4853.
10. Hall M., *Combinatorial Theory*, Braisdel Publishing Company (1967).
11. Harmuth H.F., *Transmission of Information by Orthogonal Function*, Springer-Verlag (1969).
12. Pratt W. k., *Digital Image Processing*, v.1, A Wiley-Intersciences Publication, John Wiley and Sons (1978).
13. Shovgenyuk M. V., Krokhmalskii T. Ye., Kozlovskii M. P., *Ukr. Phys. J.*, **43** (1998) 1613 (in Ukrainian).
14. Gaskill J. D., *Linear Systems, Fourier Transforms, and Optics*, John Wiley & Sons (1978).
15. Bellman R., *Introduction to Matrix Analysis*, McGraw-Hill (1960).
16. Shovgenyuk M.V., ICMP NASU, Preprint ICMP-92-25U, Lviv (1992) (in Ukrainian).
17. Shovgenyuk M.V., ICMP NASU, Preprint ICMP-92-21U, Lviv (1992) (in Ukrainian).
18. Shovgenyuk M. V., ICMP NASU, Preprint ICMP-93-22U, Lviv (1994) (in Ukrainian).
19. Shovgenyuk M. V., Hlushak P. A., *Proc. SPIE*, **2747** (1995) 468.
20. Paley R. E. A. C., *J. Math. and Physics*, **12** (1933) 311.
21. Drouin N., *Building Hadamard Matrices in Step 4 to Order 200*, U.S.Department of Commerce, NISTIR 5121 (1993).
22. Sylvester J. J., *Phil. Mag.*, **34** (1867) 461.
23. Kovalenko I. M., Hnedenko H. M., *Probability Theory*, Vyshcha shkola, Kyiv (1990) (in Russian).
24. Feller W., *An Introduction to Probability Theory and its Applications*, vol. 1, John Wiley & Sons, Chapman & Hall (1957).
25. Horn R. A., Johnson Ch. R., *Matrix Analysis*, Cambridge University Press (1986).
26. Stanley H., *Introduction to Phase Transitions and Critical Phenomena*, Clarendon Press (1971).
27. Ma S.-K., *Modern Theory of Critical Phenomena*, Benjamin (1976).
28. Shovgenyuk M. V., Krokhmalskii T. Ye., Kozlovskii M. P., ICMP NASU, Preprint ICMP-99-18U, Lviv (1999) (in Ukrainian).
29. Papoulis A., *J.Opt.Soc.Amer.*, **64** (1974) 779.
30. Ojeda-Castaneda J., Sicre E. E., *Opt. Acta*, **31** (1984) 255.
31. Shovgenyuk M. V., Krokhmalskii T. Ye., Kozlovskii M. P., *Proc. SPIE*, 3749 (1999) 689.